Computational Analysis of Permeance Prediction for Gas Separation Membrane Using Countercurrent Flow Model

MUHAMMAD AHSAN[1], THOMAS LETTENBICHLER[2]
[1]School of Chemical & Materials Engineering National University of Sciences and Technology, Islamabad 44000, PAKISTAN
[2]Management Center Innsbruck – Department of Environmental, Process & Energy Engineering, Innsbruck, AUSTRIA

Abstract: - Gas separation polymeric membranes have gained significant attention in various industries, including gas processing, petrochemicals, and environmental applications. Accurately predicting the permeance of these membranes is crucial for optimizing their design and performance. This paper presented a numerical prediction model for the permeance of a binary gas mixture under various process conditions, using only algebraic equations to minimize the calculation effort. The model considers input parameters such as feed and permeate flow rates, feed pressure, feed and permeate mole fraction, and membrane area. It demonstrates the behavior of permeance and selectivity in this study. The study also presented two case studies that utilize predicted selectivity to model counter-current flow and compare the results with experimental data from the literature. The first case study involves recovering helium from natural gas using an asymmetric high-flux membrane. The second case study separates air using nano-porous carbon as the membrane material. The numerical analysis successfully accurately predicted the permeance of gas separation polymeric membranes. The model accounted for variations in membrane thickness, feed composition, and operating conditions, providing valuable insights into the overall performance of the membrane system. It also allowed for the optimization of membrane design and operational parameters to enhance separation efficiency and productivity. The study showcased the effectiveness of numerical techniques in accurately predicting membrane performance. The developed model can be a valuable tool for membrane designers and engineers, enabling them to optimize the design and operation of gas separation systems.

Key-words: - Permeance, Numerical Modeling, Membrane Gas Separation.

Received: March 12, 2024. Revised: August 5, 2024. Accepted: September 8, 2024. Published: October 9, 2024.

1. Introduction

The industry widely uses membrane gas separation as it presents many advantages over other methods, such as cryogenic distillation or adsorption [1]. In particular, the economic efficiency of the method has been proven in natural gas treatment [2, 3]. The main advantage is that membrane gas separation does not involve a phase change, leading to less energy consumption than cryogenic distillation [4]. On the other hand, cryogenic distillation has about 90 % higher energy consumption than membrane gas separation processes [1]. Further advantages of membrane gas separation technologies are their simplicity, small footprint, and ease of scaling [1]. Nevertheless, designing a membrane application involves experimental activities to generate the required data, especially permeances [5].

Mathematical modeling in membrane gas separation is already in use. Wala-wender et al. [6]. Furthermore, Pan et al. [7] developed mathematical calculation models for different flow patterns in the seventies. Many articles about mathematical modeling in membrane gas separation have been published recently [8–11]. Until now, a prediction of the permeance is not available based on process conditions. Lee et al. developed a model for permeability prediction [12]. This mathematical model is based on the configurational entropy of the membrane and allows for predicting a specific membrane's permeability. Prabhakar et al. developed a model to predict permeability depending on temperature and rubber polymers' concentration [13]. This paper uses a mathematical model to predict permeance and selectivity –mainly based on the process conditions. The prediction is based on the partial pressure difference between the two sides of the membrane since this is the driving force in membrane gas separation [14, 15].

The predicted selectivity is used in a countercurrent model, which is solved with a finite element approach. It is more efficient than solving differential equations to calculate permeate mole fraction values than experimentally obtained values from the literature [16]. Case Study 1 compares an asymmetric high-flux membrane's values by Pan et al. that separates helium from methane [17]. The second case study compares the values from an air separation experiment by Merrit et al. using nano-porous carbon as a membrane material [18].

2. Numerical Model

As the introduction mentions, the model is based on the partial pressure difference Δp. Equation 1 shows the basic equation used to predict the permeance. The variables on the left – which describe the flux and consist of the permeate flow rate VP, the permeate mole fraction yP, and the membrane area Am – must be known. The driving force is calculated by the developed model and used with the known variable on the left side of equation 1 to predict the permeance $\bar{P}$.

$$\frac{V_P \cdot y_P}{A_m} = \bar{P} \cdot \underbrace{driving\ Force}_{\Delta p} \tag{1}$$

The partial pressure is calculated by the relation given in equation 2, in which PA is the partial pressure of species A, p is the total pressure, and xA is the mole fraction of species A.

$$P_A = p \cdot x_A \tag{2}$$

The model is derived based on the countercurrent flow pattern shown in Fig. 1 $P_{1,\,A}$, $P_{2,\,A,}$ and $P_{3,\,A,}$ are the points at which the partial pressure is calculated and represent the feed inlet, reject outlet, and permeate outlet.

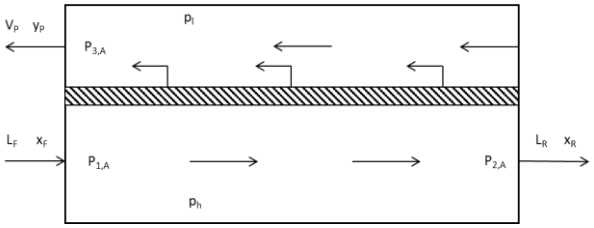

Fig. 1. Countercurrent flow model for the derivation of the equations

The following general assumptions are made for the mathematical model:

- Isothermal conditions
- There is no interaction between the different gases of the binary gas mixture
- Plug flow on the permeate and the feed side
- Steady-state conditions
- Ideal gas conditions
- The permeate is under atmospheric pressure
- Only a slight pressure drop of approximately 3 kPa occurs on the feed side

The model's basis is the overall mass and component balances, equations 3 and 4. L_F is the feed flow rate, x_F is the feed mole fraction, L_R is the reject flow rate, x_R is the reject mole fraction, V_P *is* the permeate flow rate and y_P is the permeate mole fraction.

$$L_F = L_R + V_P \tag{3}$$

$$L_F \cdot x_F = L_R \cdot x_R + V_P \cdot y_P \tag{4}$$

The partial pressures are calculated on the high-pressure side at the feed inlet and the reject outlet, equations 5 and 6. On the low-pressure side, partial pressure is required at the permeate outlet, equation 7.

$$P_{1,A} = p_F \cdot x_F \tag{5}$$

$$P_{2,A} = (p_F - p_{loss}) \cdot x_R \tag{6}$$

$$P_{3,A} = p_P \cdot y_P \tag{7}$$

The variables $P_{1,A}$ is A's partial pressure at the feed inlet, P2, A's partial pressure at the reject outlet, and P3, A's partial pressure on the permeate side.

With the definition of stage cut θ, the ratio between V_P and L_F and equations 1 and 2, the reject concentration x_R needed in equation 9, can be calculated via the component balance. The calculation of the partial pressures of component *B* follows the same scheme; since this model deals only with binary gas mixtures, the concentration of *B* in the feed is defined by 1 – x_F, and so on for permeate and reject. This procedure leads to equations 8, 9, and 10, which calculate B's partial pressures.

$$P_{1,B} = p_F \cdot (1 - x_F) \tag{8}$$

$$P_{2,B} = (p_F - p_{loss}) \cdot (1 - x_R) \tag{9}$$

$$P_{3,B} = p_P \cdot (1 - y_P) \tag{10}$$

As the next step, the differences between A and B's partial pressures are calculated separately because these are the driving forces in membrane gas separation. Thus, equations (*11)* and (*12)* are the pressure differences between P_1 and P_3 and P_2 and P_3, respectively.

$$\Delta p_{1,3} = P_1 - P_3 \tag{11}$$

$$\Delta p_{2,3} = P_2 - P_3 \tag{12}$$

The mean driving force across the membrane is calculated using the average of equations 11 and 12.

$$\bar{P}_A = \frac{V_P \cdot y_P}{A_m \cdot \Delta p_{av,A}} \tag{13}$$

$$\bar{P}_B = \frac{V_P \cdot (1 - y_P)}{A_m \cdot \Delta p_{av,B}} \tag{14}$$

Since the permeate flow, the membrane area, and the permeate mole fraction are input parameters, and the developed model calculates the mean partial pressure difference, all variables from equation (1) are known. Hence, the permeance for *A* and *B* can be calculated with equations 13 and 14, respectively. $\bar{P}_A$ is the permeance of component *A*, $\bar{P}_B$ is the permeance of component *B*. The selectivity or ideal separation factor α^* is calculated using the ratio between equations 13 and 14.

Since some approximations are applied to the model, such as atmospheric pressure on the low-pressure side, the permeate mole fraction used in the mass balance and an input parameter cannot be directly used to calculate the permeances. Also, the permeate mole fraction at the right edge of the membrane application is unknown and must be first estimated. Therefore, an additional permeate mole fraction variable y'_P is introduced, calculated by multiplying y_P – the permeate mole fraction used initially – with a factor *c*. Factor *c* is varied from 0 to 1. At the end of each calculation loop – after the permeances and the selectivity are calculated with a certain y'_P – the selectivity is used as input in the quadratic equation (general solution in membrane gas separation) to calculate the corresponding permeate mole fraction. As the last step, the difference between the result of the quadratic equation and y'_P is calculated. This difference is the loop criteria. As soon as the difference is smaller than 10^{-3}, the loop stops, and the calculation is completed.

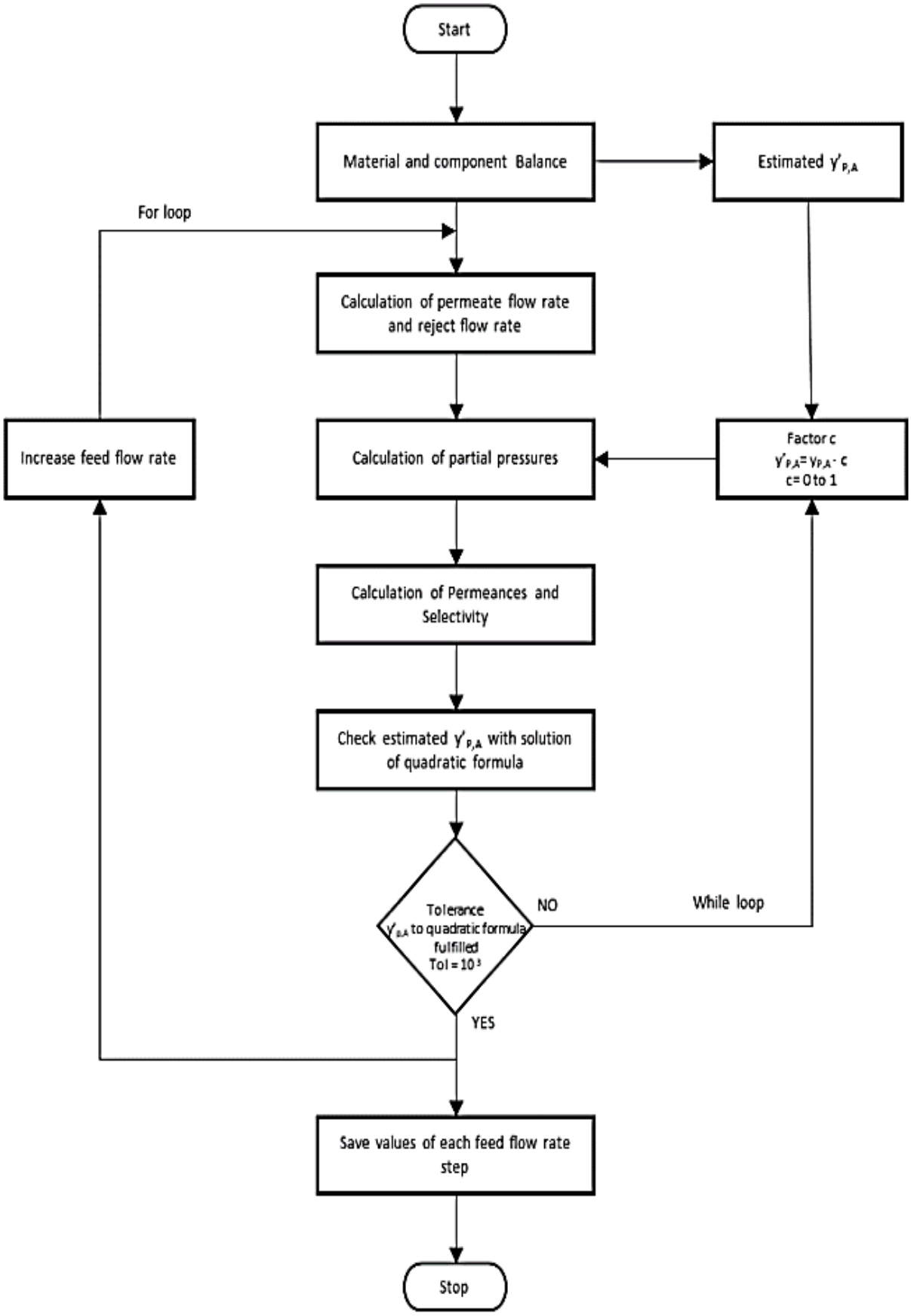

Fig. 2. Flow chart for feed flow rate loop.

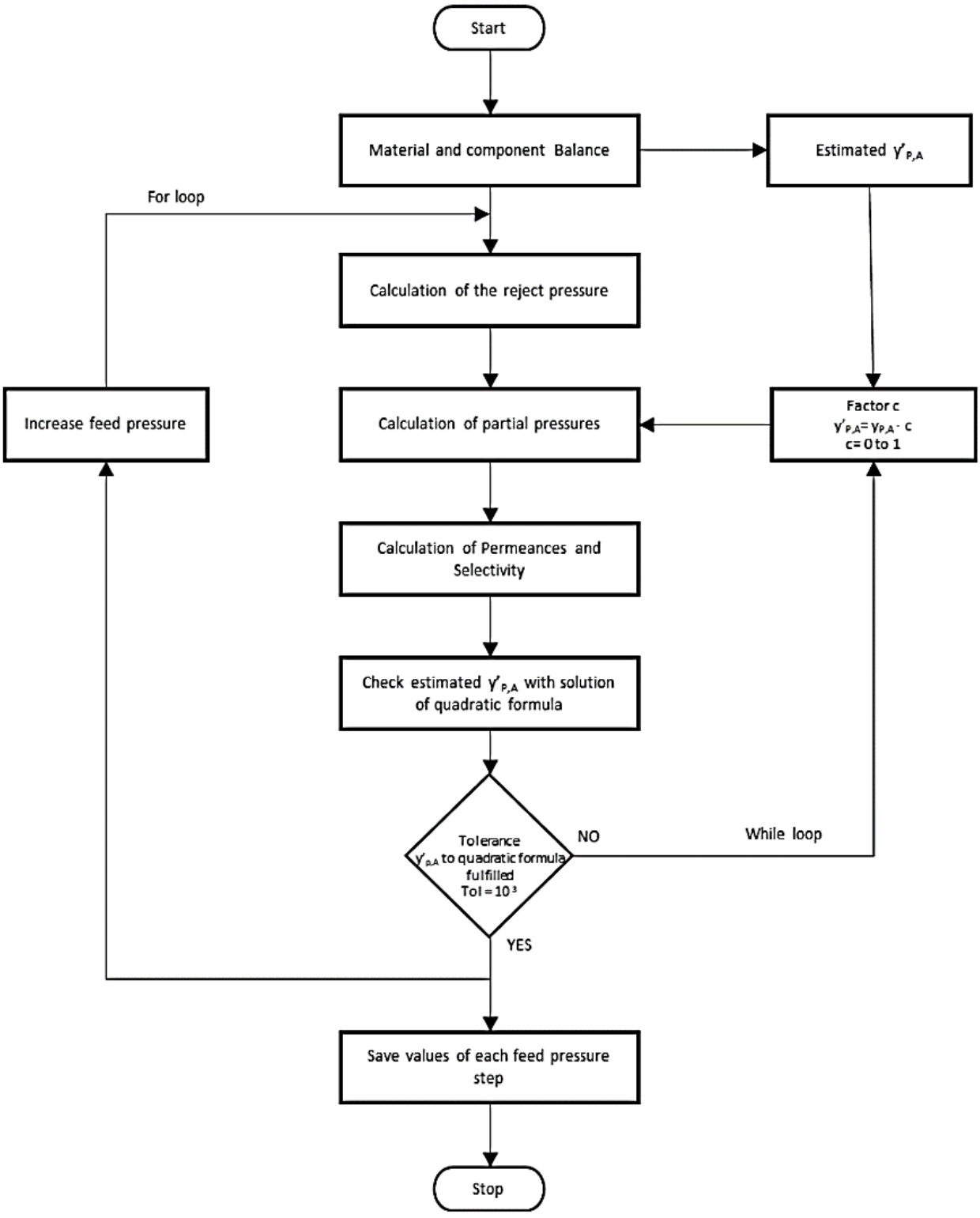

Fig. 3. Flow chart for feed pressure loop.

Applying an additional loop in which the previous loop is nested, the behavior of permeance and selectivity under changing process conditions can be investigated to the feed pressure or feed flow rate. The flow charts of these two programs are shown in Fig. 2 and Fig. 3, respectively. After predicting the permeance and selectivity, it is used as input for a countercurrent flow model. The countercurrent flow model is taken from Ahsan et al. and Geankoplis [16, 19]. As a result, the model's permeate mole fractions and the reference values are compared.

3. Results and Discussion

3.1 The behavior of permeance and selectivity

The input parameters for the problem are taken from the literature [5]. In the reference, the permeability of species A is given with 500×10-10 cm³·cm/(s·cm²·cm Hg) and the selectivity with 10. A comparison of the reference and the simulated values is shown in Table I.

The feed pressure used for this comparison is 253 kPa, and the feed flow rate is 106 cm³/s. Also, a feed mole fraction of

0.209, a stage cut of 0.4, a membrane area of 6.9×108 cm² and a permeate mole fraction of 0.45 are input parameters for the calculation. The main challenge is that the permeate mole fraction on the right edge of the membrane application is unknown; therefore, this value is initially estimated. The mathematical algorithm described in section 2 shows that the permeate mole fraction on the right edge is calculated iteratively—finally, the feed flow rate and the feed pressure increase after each calculation loop.

The effect of increasing the feed flow rate on the permeances is shown in Fig. 4. Again, a linear influence on both permeances is observed. Whereby the permeance ratio remains constant, leading to a constant selectivity. This behavior is consistent because selectivity is assumed to be a membrane material property. By changing the feed pressure, the behavior differs from changing the feed flow rate. The variation of the feed pressure has a potential influence on the permeances and selectivity. The results are shown in Fig. 5 and Fig. 6 for the permeances and the selectivity, respectively.

TABLE I. PERMEANCE AND SELECTIVITY VALUES WERE OBTAINED WITH THE DEVELOPED MATHEMATICAL MODEL

Variable	Unit	Model result	Literature [5]	Difference (%)
$\bar{P}_A$	Barrer/cm	2.2×10^{-5}	2.0×10^{-5}	10.0
$\bar{P}_B$	Barrer/cm	1.8×10^{-6}	2.0×10^{-6}	10.0
α*	-	12.4	10.0	24.0

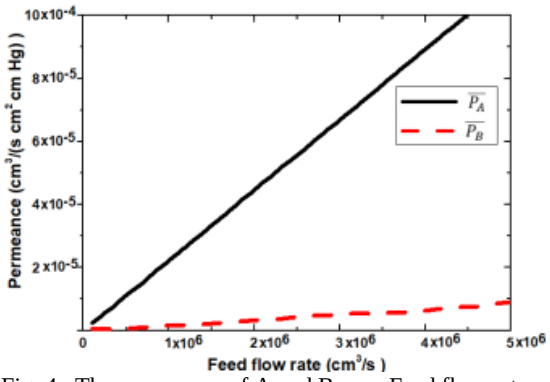

Fig. 4. The permeance of A and B over Feed flow rate, with x_F=0.209, p_F=253 kPa, θ=0.4, A_m=6.9×10⁸ cm², and y_P=0.45.

3.2 Case Study I: Helium recovery

Helium is mainly required for its chemically inert properties, low density, and cryo-genic applications [20]. These properties make it worth separating it from natural gas. Helium-rich natural gas consists of up to 4 % Helium [20]. This case study deals with separating a binary mixture of helium and methane. The other components of natural gas are not considered in the simulation. The selectivity is first predicted and then used as input in a countercurrent model. The numerically calculated permeate mole fraction values obtained by the developed mathematical model are compared with the generated values from Pan et al. [17]. The developed model predicts the selectivity with 66.4 and uses these values as input in the countercurrent flow model, solved using a finite element approach [5, 16]. As input parameters, a stage cut of 0.23, a permeate mole fraction of 0.9863, a pressure ratio of 0.05, and a feed mole fraction of 0.6 is used [16]. A pressure ratio of 0.05 leads to a feed pressure of 2027 kPa because on the permeate side, 1 atmosphere is assumed. The result is shown in Fig. 7; the solid line is the mathematical model, and the triangles refer to the reference values from Pan et al. [17].

The developed model's result fits the experiment's data quite well. However, in the end (at low xR values), the experimental data are slightly higher than those calculated with the developed mathematical model. A comparison is shown in Table II.

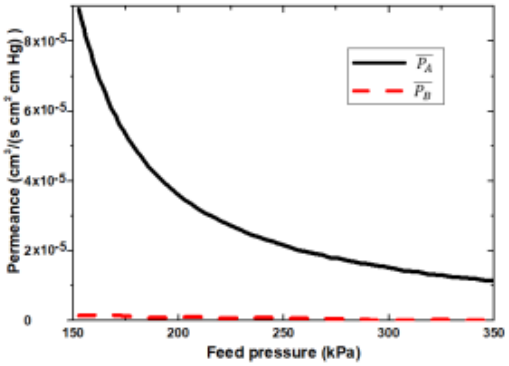

Fig. 5. The permeance of A and B over feed pressure, with x_F=0.209, L_F=1×10⁶ cm³/s, θ=0.4, A_m=6.9×10⁸ cm², and y_P=0.45.

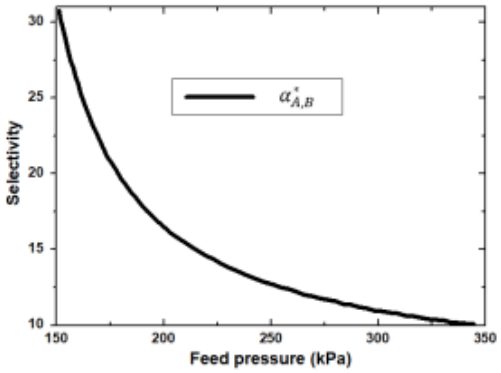

Fig. 6. The selectivity of A and B over feed pressure, with x_F=0.209, L_F=1×10⁶, θ=0.4, A_m=6.9×10⁸ cm², and y_P=0.45.

TABLE II. COMPARISON BETWEEN THE MATHEMATICAL MODEL AND REFERENCE VALUES.

x_R	y_P model	y_P [17]	Difference (%)
0.03	0.9415	0.9211	2.2
0.06	0.9573	0.9414	1.7
0.085	0.9636	0.9512	1.3
0.12	0.9689	0.9602	0.9
0.24	0.9779	0.9754	0.25
0.48	0.9863	0.9863	0.0

3.3 Case Study II: Air separation

The calculation assumes that the feed mole fraction of O2 and N2 are 0.198 and 0.802, respectively. Thus, all other components usually present in the air are neglected in the simulation. The experiment is carried out by Merrit et al. at a feed pressure of 413.7 kPa and uses nanoporous carbon as membrane material [18].

The developed model predicts a selectivity of 6.3 and is used as input in the countercurrent model. As input values for predicting a stage cut of 0.01, a permeate mole fraction of

0.479 and a feed mole fraction of 0.198 are used. The results are shown in Fig. 8 and Table 3. The values calculated with the model are compared with the experimentally determined values of Merrit et al. [18]. However, the result is somewhat worse than the results of Case Study I. This is mainly due to the higher feed pressure in Case Study I. The higher feed pressure compensates better for the assumed atmospheric pressure on the low-pressure side.

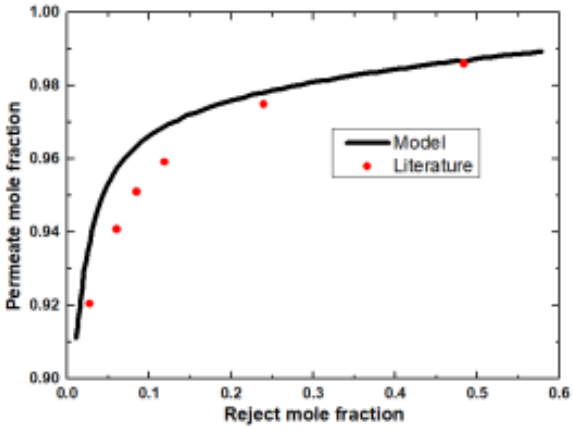

Fig. 7. The selectivity is predicted with a stage cut of 0.23, a permeate mole fraction of 0.986, a pressure ratio of 0.05, and a feed mole fraction of 0.6. The solid line is the developed mathematical model's solution, and the triangles are the reference values [17].

TABLE III. COMPARISON BETWEEN THE MATHEMATICAL MODEL AND REFERENCE VALUES.

θ	**y_P model**	**y_P [18]**	**Differences (%)**
0.01	0.449	0.479	6.3
0.13	0.421	0.421	0.0
0.27	0.385	0.363	6.1
0.31	0.375	0.347	8.1
0.40	0.351	0.326	7.7
0.47	0.332	0.302	9.9
0.65	0.283	0.266	6.4

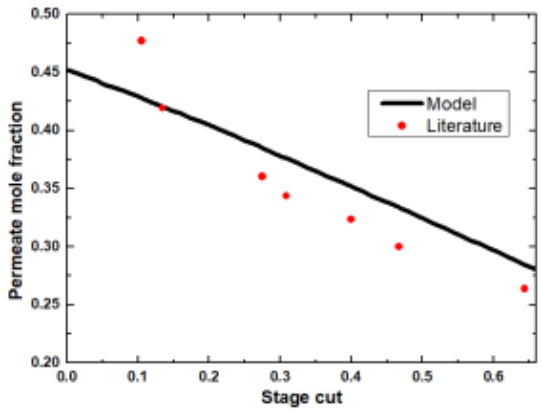

Fig. 8. Results of Case Study II. The triangles refer to the experimentally obtained permeate mole fractions by Merrit et al. [18].

4. Conclusion

The comparison in the Case Studies shows that the developed model calculates permeate mole fractions comparable to those given by Pan et al. and Merrit et al. [17, 18]. The results obtained in Case Study 1 are slightly better than those obtained from Case Study 2. This is mainly due to the higher feed pressure in Case Study 1. The higher feed pressure compensates better for the assumption of atmospheric pressure on the permeate side, leading to better results in Case Study 1. In part 1, the behavior of permeance and selectivity was investigated by changing the feed flow rate and pressure. The results show that increasing the feed flow rate leads to a linear increase in permeance. The ratio between the two permeances remains constant, which results in a constant selectivity. This behavior is expected, as selectivity is assumed to be a material property of the membrane and should not be influenced by the feed flow rate. A change in the feed pressure leads to a potential behavior of both permeances and selectivity. The selectivity decreases with increasing feed pressure. The examination of equations 13 and 14 shows a $1/\Delta p$ relationship that leads to the observed behavior observed in Fig. 5 and Fig. 6. Since the molar fraction of the permeate is an input parameter and must be known in advance, an experiment to determine the permeate composition is necessary; therefore, it would be great to improve the model to eliminate the permeate mole fraction parameter. This model is only able to deal with binary gas mixtures. However, dealing with multi-component mixtures for industrial applications would be interesting because most gas streams consist of more than two components. Therefore, extending this model to a multi-component mixture would be meaningful. Also possible would be a coupling of different mathematical models, like the thermodynamic model from Lee and coworkers [12] or the temperature dependency model of Prabhakar et al. [13], to improve the accuracy and scope of the mathematical models.

LIST OF ABBREVIATIONS

L_F	Feed flow rate
L_R	Reject flow rate
V_P	Permeate flow rate
x_F	Feed mole fraction
x_R	Reject mole fraction
y_P	Permeate mole fraction
P_1	Partial pressure at the feed inlet
P_2	Partial pressure at the reject outlet
P_3	Partial pressure on the permeate side
Δp	Partial pressure difference
Δp_{av}	Mean partial pressure difference along the membrane
p_F	Feed pressure
p_P	Permeate pressure
p_{loss}	Pressure drop on the high-pressure side
$\bar{P}$	Permeance
α^*	Selectivity
θ	Stage cut
A_m	Membrane area

References

[1] C. Z. Liang, T.-S. Chung, and J.-Y. Lai, "A review of polymeric composite membranes for gas separation and energy production," Progress in Polymer Science, vol. 97, p. 101141, 2019.

[2] H. Vinh-Thang and S. Kaliaguine, "Predictive models for mixed-matrix membrane performance: a review," Chemical reviews, vol. 113, no. 7, pp. 4980-5028, 2013.

[3] M. T. Ravanchi, T. Kaghazchi, and A. Kargari, "Application of membrane separation processes in petrochemical industry: a review," Desalination, vol. 235, no. 1-3, pp. 199-244, 2009.

[4] P. Bernardo, E. Drioli, and G. Golemme, "Membrane gas separation: a review/state of the art," Industrial & engineering chemistry research, vol. 48, no. 10, pp. 4638-4663, 2009.

[5] D. Coker, B. Freeman, and G. Fleming, "Modeling multicomponent gas separation using hollow‐fiber membrane contactors," AIChE journal, vol. 44, no. 6, pp. 1289-1302, 1998.

[6] Q. Qian et al., "MOF-based membranes for gas separations," Chemical reviews, vol. 120, no. 16, pp. 8161-8266, 2020.

[7] R. Khalilpour, K. Mumford, H. Zhai, A. Abbas, G. Stevens, and E. S. Rubin, "Membrane-based carbon capture from flue gas: a review," Journal of Cleaner Production, vol. 103, pp. 286-300, 2015.

[8] J. Marriott, E. Sørensen, and I. Bogle, "Detailed mathematical modelling of membrane modules," Computers & Chemical Engineering, vol. 25, no. 4-6, pp. 693-700, 2001.

[9] H. J. Jung, S. H. Han, Y. M. Lee, and Y.-K. Yeo, "Modeling and simulation of hollow fiber CO 2 separation modules," Korean Journal of Chemical Engineering, vol. 28, pp. 1497-1504, 2011.

[10] S. Lock, K. Lau, I. L. S. Mei, A. Shariff, Y. Yeong, and A. Bustam, "Molecular simulation and mathematical modelling of glass transition temperature depression induced by CO2 plasticization in Polysulfone membranes," in IOP Conference Series: Materials Science and Engineering, 2017, vol. 226, no. 1: IOP Publishing, p. 012172.

[11] A. Ebadi Amooghin, S. Mirrezaei, H. Sanaeepur, and M. M. Moftakhari Sharifzadeh, "Gas permeation modeling through a multilayer hollow fiber composite membrane," Journal of Membrane Science and Research, vol. 6, no. 1, pp. 125-134, 2020.

[12] D. K. Lee, Y. W. Kim, K. J. Lee, B. R. Min, and J. H. Kim, "Thermodynamic model of gas permeability in polymer membranes," Journal of Polymer Science Part B: Polymer Physics, vol. 45, no. 6, pp. 661-665, 2007.

[13] R. S. Prabhakar, R. Raharjo, L. G. Toy, H. Lin, and B. D. Freeman, "Self-consistent model of concentration and temperature dependence of permeability in rubbery polymers," Industrial & engineering chemistry research, vol. 44, no. 5, pp. 1547-1556, 2005.

[14] R. Smith, Chemical process: design and integration. John Wiley & Sons, 2005.

[15] J. Smith, W. McCabe, and e. Peter Harriott, Unit Operations of Chemical Engineering. McGraw-Hill Education, 2004.

[16] M. Ahsan and A. Hussain, "Mathematical modelling of membrane gas separation using the finite difference method," Pacific Science Review A: Natural Science and Engineering, vol. 18, no. 1, pp. 47-52, 2016.

[17] C. Pan, "Gas separation by permeators with high‐flux asymmetric membranes," AIChE journal, vol. 29, no. 4, pp. 545-552, 1983.

[18] A. Merritt, R. Rajagopalan, and H. C. Foley, "High performance nanoporous carbon membranes for air separation," Carbon, vol. 45, no. 6, pp. 1267-1278, 2007.

[19] C. Geankoplis, Transport processes and separation (Process Principles, Prentice Hall NJ). 2003.

[20] C. A. Scholes and U. Ghosh, "Helium separation through polymeric membranes: selectivity targets," Journal of Membrane Science, vol. 520, pp. 221-230, 2016.

Contribution of Individual Authors to the Creation of a Scientific Article (Ghostwriting Policy)

The authors equally contributed in the present research, at all stages from the formulation of the problem to the final findings and solution.

Sources of Funding for Research Presented in a Scientific Article or Scientific Article Itself

No funding was received for conducting this study.

Conflict of Interest

The authors have no conflicts of interest to declare that are relevant to the content of this article.